

# QUINTESSENTIAL COSMOLOGY AND COSMIC ACCELERATION

PAUL J. STEINHARDT  
*Department of Physics*  
*Princeton University*

## 1. Introduction

Quintessence [1, 3] and the cosmological constant [4] are unanticipated and unwanted energy components from the point-of-view of both cosmologists and high energy physicists. Yet, confirming either would undoubtedly be one of the most important discoveries in both fields and would produce new links between the two.

For cosmology, the discovery of a new energy component would finally balance the energy budget, making the total energy content of the universe equal to the critical density predicted by inflation [5, 6, 7, 8]. The fact that the energy component has negative pressure and causes the universe to accelerate has a subtle but numerically significant impact on the past evolution of the universe and large-scale structure formation, resolving numerous difficulties with the standard cold dark matter model. The dramatic impact is on the future history of the universe. For decades, the common view was that the universe is decelerating due to the self-gravitation of matter and radiation. The only issue seemed to be whether the deceleration is sufficient to halt the expansion and cause the universe to contract to a big crunch, or whether the deceleration is too meager and the universe continues to expand at a slower and slower rate. Now, the evidence indicates that neither scenario is correct. The expansion is speeding up, driven by a mysterious form of dark energy that will ultimately overwhelm the universe.

For fundamental physics, quintessence or a cosmological constant represents new, ultra-low energy phenomena beyond the standard model. If firmly established by future observations, the discovery will be recognized as a fantastic, valuable hint about the ultimate, unified theory. The fact that the component can be probed observationally is an added bonus, especially since many predictions of unified theories entail high energies beyond

the realm of experiment.

Moreover, just as the Copernican revolution changed forever the view of our place in the universe, the discovery of cosmic acceleration will change the view of our place in time. In the static universe picture, what we see in the universe today is representative of the universe as it always has been and always will be. In the big bang picture, the universe has been undergoing steady evolution from a simple, uniform, cosmic soup of elementary particles to ever more complex structure, in close analogy to biological evolution. The view of the universe emerging today is that the universe as we know it is only a brief interlude between two periods of cosmic acceleration powered by negative pressure, inflation at early times and now acceleration once again. Life, the stars, the galaxies, and large-scale structure are completely ephemeral phenomena in the course of cosmic history, a momentary spark in an accelerating universe.

The evidence for cosmological acceleration is presented in Sec. II. We show how three distinct types of observations currently indicate cosmic acceleration. In Sec. III, we turn to the two competing theoretical explanations for explaining what powers the cosmic acceleration: either an inert vacuum density (or cosmological constant) or a dynamical, quintessence component. We focus particularly on the progress that has been made in developing quintessence from a rather artificial and ill-defined concept into a promising and well-motivated possibility. Perhaps the most important motivation for considering quintessence is the cosmic coincidence problem: why has cosmic acceleration begun at this particular moment in cosmic history? If acceleration had begun a little earlier, structure would never have formed in the universe, and, if acceleration had begun a little later, we would not detect it today. For this timing of the acceleration to occur, it must be that the matter density and dark energy density just happen to coincide (nearly) today even though they decrease at substantially different rates as the universe expands. The cosmological constant proposal offers little insight into the coincidence. However, some very promising ideas have emerged from the study of quintessence – tracker fields and creeper fields – which partially address the coincidence problem. In Sec. IV, the current observational status of quintessence will be summarized, and the future prospects for distinguishing quintessence from a cosmological constant will be discussed. In Sec. V, we outline some of the remaining theoretical challenges.

## **2. The evidence for cosmic acceleration**

The most impressive aspect of the case for cosmic acceleration is that three separate lines of evidence have arisen which simultaneously lead

us to the same startling conclusion [9]. Although the supernovae results [10, 11, 12, 13] are what first captured the attention of the broad scientific community, strong evidence already existed beforehand [19] and other kinds of measurements may ultimately provide the most reliable test in the future.

*Direct evidence of accelerated expansion:* Accelerated expansion produces a systematic deviation from the linear Hubble law at large red shift. Attempts to measure the deceleration parameter and higher order non-linearities have been a goal of cosmology for decades, and promising techniques have been explored, only to be foiled by unforeseen evolutionary effects. The latest approach, using Type IA supernovae as standard candles, appears promising from both a theoretical and empirical view at present. The results of the Supernovae Cosmology Project [10, 14, 15] are summarized in Figure 1; a competing group, the High- $z$  Supernovae group [11, 12, 16, 17], uses somewhat different methods and achieves a similar result. Both groups find that distant supernovae are significantly fainter (by nearly half a magnitude) compared to a sample of nearby supernovae than would be expected in a cosmological model with  $\Omega_m = 1$ , such as the standard cold dark matter (SCDM) model. The SCP group reports  $\Omega_m = 0.28 \pm 0.8 \pm 0.5$  assuming a flat universe ( $\Omega_m + \Omega_\Lambda = 1$ ) [10]. (Allowing non-zero curvature, the constraint is  $0.8\Omega_m - 0.6\Omega_\Lambda = -0.2 \pm 0.1$ .) ( $\Omega_i$  is the ratio of the energy density in component  $i$  to the critical density,  $\rho_c = 8\pi G/3H_0^2$ , where  $H_0 = 100h$  km s $^{-1}$  Mpc $^{-1}$ . We use  $i = m$  for the total (baryonic and nonbaryonic) matter density,  $i = b$  for the baryon density,  $i = r$  for the radiation density,  $i = \Lambda$  for the cosmological constant or vacuum density, and  $i = Q$  for quintessence.) Although the results are impressive, one should recall the sorry history of past attempts at long-distance, standard candles: in a nutshell, the initial, small statistical errors are ultimately replaced by large systematic uncertainties. In the case of Type IA supernovae, the most worrisome aspects are that the luminosity of supernovae may evolve with red shift in such a way as to mimic the predictions of accelerated expansion [18] or that dust at large red shift may make supernovae appear fainter than expected for a decelerating universe. Considerable efforts are already underway to test these possibilities.

If confirmed, cosmic acceleration can be interpreted as evidence for a substantial cosmic energy component with negative pressure. According to Einstein's theory of general relativity, the scale factor  $a(t)$ , which represents the expansion of the universe as a function of time, satisfies the differential equation:

$$\ddot{a} = -\frac{4\pi G}{3}(\rho + 3p)a \quad (1)$$

where  $G$  is Newton's constant,  $\rho$  is the energy density, and  $p$  is the pressure.

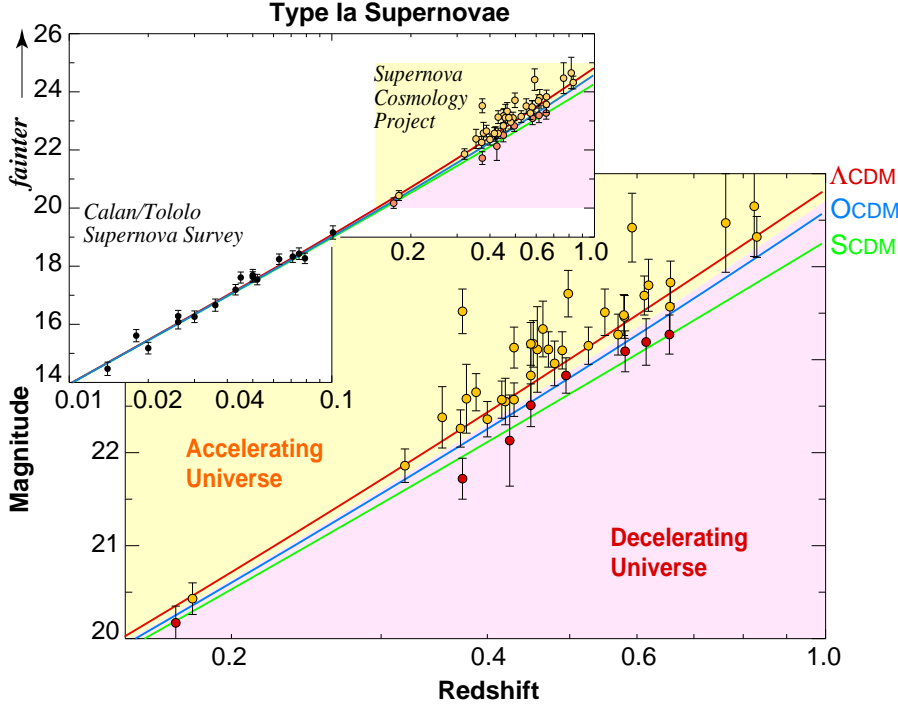


Figure 1. Observed brightness (magnitude) vs. red shift for Type Ia supernovae observed at low red shift by the Calan-Tololo Supernova Survey and at high red shift by the Supernova Cosmology Project (SCP) (with  $1\sigma$  error bars) compared with model expectations. The standard cold dark matter model (SCDM) has  $\Omega_m = 1$ ; OCDM is the best-fit open model and has  $\Omega_m = 0.3$ ; and  $\Lambda$ CDM is a flat model with  $\Omega_m = 0.3$  and  $\Omega_\Lambda = 0.7$ . The effect of a cosmological constant accelerating the expansion rate (as in  $\Lambda$ CDM) is seen as a relative ‘dimming’ of the distant SNIa compared to decelerating models. Similar results have been found by the High-Z Supernovae team (Riess *et al.*).

Baryonic and nonbaryonic cold dark matter are essentially pressureless, and radiation has positive pressure,  $p = \rho/3$ . If the universe contains only these energy components, then, according to Eq. (1), the universe is decelerating,  $\ddot{a} < 0$ . Note that this equation does not include explicitly the spatial curvature, so deceleration occurs whether the universe is open, flat, or closed if the pressure is non-negative. If the universe is found to be accelerating, there must be an energy component  $\rho_Q$  with negative pressure  $p_Q$  such that  $\rho_{tot} + 3p_{tot} < 0$ , or  $p_{tot} < -\rho_{tot}/3 < 0$ , where  $\rho_{tot}$  is the total energy density. Since  $\rho_Q + p_Q \geq 0$  for any physically plausible negative pressure component  $\rho_Q$  (the positive energy condition), then  $\rho_Q$  must be at least one-third

the total energy density,  $\rho_Q > \rho_{tot}/3$  (assuming all other components have non-negative pressure) in order for  $\ddot{a}$  to be greater than zero.

*Evidence for a flat, low-density universe — “Cogito ergo sum”*: A strong case for a negative pressure component already existed and was presented forcefully several years ago [19], well before the supernovae data indicated an accelerating universe [15]. The argument relies on combining three observed features of the universe and an argument I entitle “cogito, ergo sum.” First, the argument rests on the observation that the total mass density of the universe is less than the critical density predicted for a flat universe. While the observations were controversial for many decades, today at least eight different methods of constraining the mass density exist: cluster abundance, cluster abundance evolution, the mass-to-light (M/L) test,  $\Gamma \equiv \Omega_m h$  as determined by large-scale structure, baryon fraction based on x-ray observations of clusters, gravitational lensing of massive clusters, and the age of the universe as inferred from globular clusters compared to the Hubble age determined from measurements of the Hubble parameter [21, 22, 9, 20]. Remarkably, all eight methods agree that the mass density is less than half the critical value [19, 20]. It is difficult to imagine so many different measurements with different systematic uncertainties reversing themselves to recover a good fit to an Einstein-de Sitter ( $\Omega_m = 1$ ) universe.

The second assumed feature is that the universe is flat. Some would argue that flatness is a necessary condition based on confidence in inflationary cosmology (for which other evidence exists) or based on the classical flatness-problem argument [23]. Fortunately, the issue can be decided by observation rather than relying on theoretical arguments alone. The key observational test is the angular scale or, equivalently, the multipole moment ( $\ell$ ) of the first acoustic peak in the cosmic microwave background (CMB) temperature anisotropy power spectrum [26]. The power spectrum is the Legendre transform of the CMB temperature angular autocorrelation function. The shape of the power spectrum as a function of  $\ell$  is an extraordinarily sensitive test of cosmological models and their parameters. A prominent feature is a series of peaks resulting from acoustic oscillations of the baryon-photon cosmic fluid. See Figure 2. The oscillations are caused by density perturbations, such as those created during inflation. In the case of inflation, if the density can be decomposed into a sum of fourier modes with different comoving wavelengths, then comoving wavelengths longer than the Hubble horizon are frozen at some amplitude. When the sound horizon grows to be comparable to the wavelength, the mode begins to oscillate. The oscillation is due to a combination of gravity, which causes the amplitude to grow as baryons are drawn together in regions of high density, and the pressure of the baryon-photon fluid which pushes the baryons apart when the amplitude is too high. In measuring the tempera-

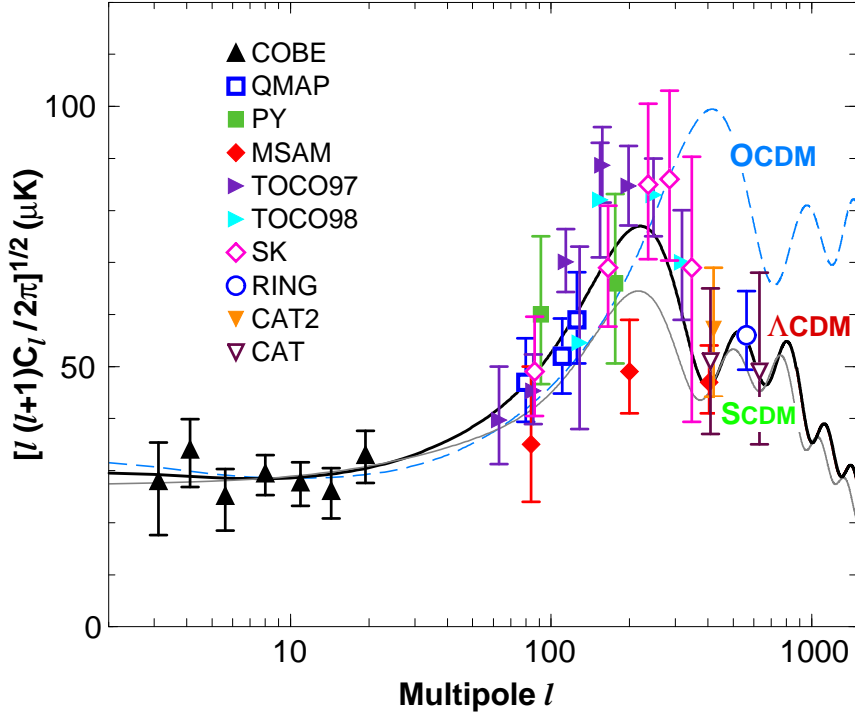


*Figure 2.* The cosmic microwave background temperature anisotropy power spectrum is shown as a function of angular scale. The multipole  $\ell$  corresponds roughly to an angular scale of  $\pi/\ell$  radians. Flat models ( $\Omega_m + \Omega_\Lambda = 1$ ), such as the standard cold dark matter (SCDM) model with  $\Omega_m = 1$  and the best-fit  $\Lambda$ CDM model with  $\Omega_m = 0.3$ , produce an acoustic peak at  $\ell \approx 200$  (about one degree on the sky). Shown also is the predicted anisotropy power spectrum for the best-fit open (OCDM) model with adiabatic fluctuations.

ture anisotropy on different angular scales, one is probing different modes at different stages of compression and rarefaction. The first acoustic peak corresponds to the mode undergoing its first compression; that is, the mode whose wavelength is equal to the sound horizon at recombination. The magnitude of the sound horizon is relatively insensitive to most cosmological parameters, and, so, can serve as a kind of “standard ruler.” If space is flat, then it is straightforward to show that the angle subtended by this standard ruler on the last scattering surface as seen on the sky today is about 1 degree (or  $\ell_{flat} \approx 220$ ). If space is curved (open or closed), the path of light from the last scattering surface to our detectors is distorted so as to change the apparent subtended angle. For example, in an open universe, the sound horizon subtends a smaller angle so that the maximum of the first acoustic peak lies at a substantially larger value of  $\ell \approx \ell_{flat}(\Omega_m)^{-1/2}$ .

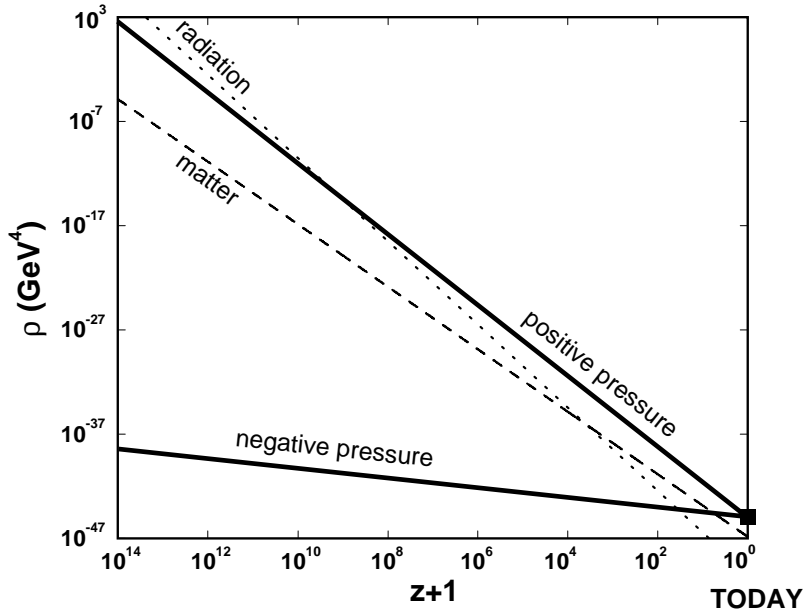


*Figure 3.* Pressure versus red shift plot indicating the evolution of the matter and radiation density compared to a dark energy component with either positive or negative pressure. According to observations, the dark energy dominates the matter and radiation energy density today (solid square). If the dark energy has positive pressure in the past, as well. Since the matter density never dominates, it is impossible to form large scale structure. On the other hand, dark energy density with negative pressure becomes negligible compared to the matter density in the past, allowing a finite range of time between  $z = 10^4$  and  $z \approx 1$  where matter dominates and structure can form.

Hence, measuring the angle is the most promising method for determining whether the universe is flat. Already five years ago, with less CMB data in hand than we have today, the best-fit (adiabatic) open model did not fit the combination of CMB and cluster abundance constraints at an acceptable level [19]; the misfit is statistically much more significant today [9].

If subcritical density and flatness are accepted as properties of our universe, then the only other feature one must assume to prove cosmic acceleration is that we exist: *cogito, ergo sum*. I think, therefore, I am. And, if I am, there must be an earth for me to stand on, a sun to shine over me, a galaxy to make the sun, and clustering matter on cosmic scales to make the galaxy.

How do the three features — subcritical mass density, flatness, and clus-

tered matter – combine to imply a negative pressure component? Consider Figure 3, which shows a plot of energy density versus red shift ( $z$ ). The figure shows the matter and radiation density falling at different rates owing to the fact that they have different equations-of-state,  $w \equiv p/\rho$ . Radiation has  $w = 1/3$  and matter has  $w = 0$ . For constant  $w$ , the scale factor grows as  $a(t) = t^{2/[3(1+w)]}$  and the energy density decreases as  $\rho \propto a^{-3(1+w)}$ . Now suppose that the matter and radiation density are less than half the critical density, and the universe is flat, as current data suggests. Then, there must be an additional dark energy component that dominates the universe today. If the component has positive pressure, then the energy density in this component decreases more rapidly than the matter density so that the slope in Figure 3 is more negatively steeped than the matter density. Extrapolating backwards in time, the component dominates the matter density not only today, but forever in the past. With gravity alone, structure growth is a delicate balance between the effect of inhomogeneity drawing matter together and expansion spreading the matter. Only during the period when  $\Omega_m \approx 1$  does the first effect win and structure grow appreciably. In the positive pressure case, since matter never dominates, it is not possible to form the non-linear structures (galaxies, clusters, etc.) observed throughout the universe beginning from the tiny fluctuations observed by the COBE satellite experiment [28]. (In this case, structure could not grow by gravitational instability alone, but would require an additional long-range force or some other new physics.) On the other hand, if the pressure is negative, the energy density decreases more slowly than the matter density. Extrapolating backwards in time, a negative pressure component that dominates the universe today becomes subdominant to the matter density at some time in the past. If the component has a *sufficiently* negative  $w$ , the matter will dominate for a long enough period to form the observed structure via gravitational stability beginning from the tiny fluctuations measured in the cosmic microwave background anisotropy. To account for the observed structure, sufficiently negative means  $w < -0.33$  [19, 20], which corresponds to the regime in which the expansion of the universe is accelerating. Hence, we see that evidence of subcritical matter density and flatness, combined with existence of structure, is sufficient to prove the case for a negative pressure component and, an accelerating universe. (The argument as presented here assumes  $w$  is constant or changing slowly; a more detailed discussion is required to dispose of cases where  $w$  is changing rapidly for a component, as in the case of decaying dark matter. This is left as an exercise for the reader.)

*Evidence for a high acoustic peak in the cosmic microwave background power spectrum:* The most recent and, statistically, the weakest evidence for a negative pressure component is based on measuring the height of the first



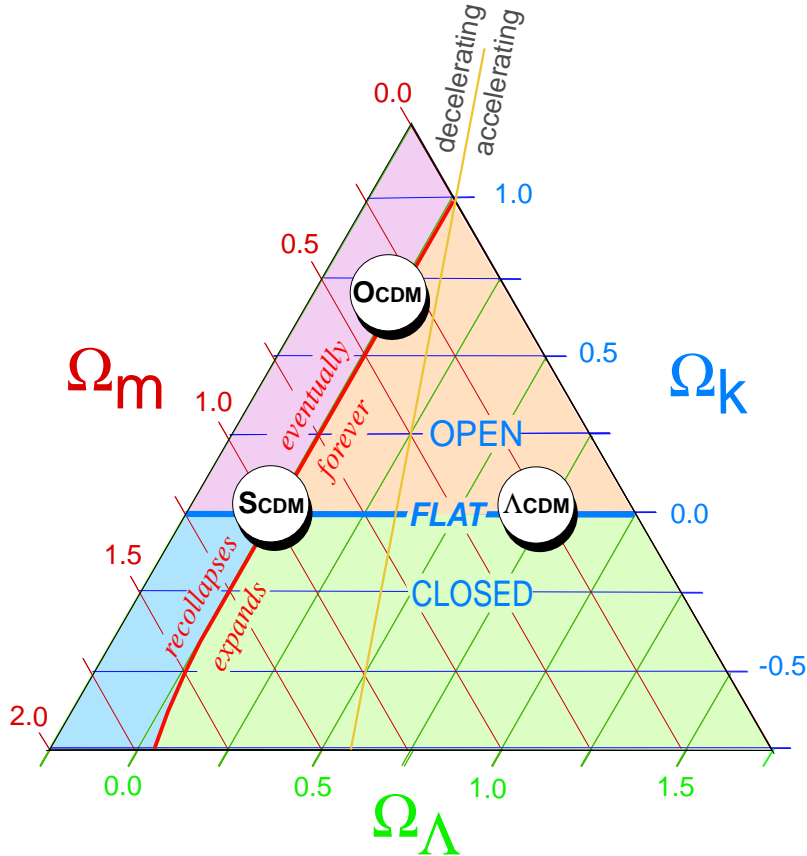


*Figure 4.* The triangle plot represents the three key cosmological parameters –  $\Omega_m$ ,  $\Omega_\Lambda$ , and  $\Omega_k$  – where each point in the triangle satisfies the sum rule  $\Omega_m + \Omega_\Lambda + \Omega_k = 1$ . The central horizontal line (marked Flat) corresponds to a flat universe ( $\Omega_m + \Omega_\Lambda = 1$ ), separating an open universe from a closed one. The diagonal line on the left (nearly along the  $\Lambda = 0$  line) separates a universe that will expand forever (approximately  $\Omega_\Lambda > 0$ ) from one that will eventually recollapse (approximately  $\Omega_\Lambda < 0$ ). And the light-gray, nearly vertical line separates a universe with an expansion rate that is currently decelerating from one that is accelerating. The location of three key models are highlighted: standard cold-dark-matter (SCDM) is dominated by matter ( $\Omega_m = 1$ ) and no curvature or cosmological constant; flat ( $\Lambda$ CDM), with  $\Omega_m = 1/3$ ,  $\Omega_\Lambda = 2/3$ , and  $\Omega_k = 0$ ; and Open CDM (OCDM), with  $\Omega_m = 1/3$ ,  $\Omega_\Lambda = 0$  and curvature  $\Omega_k = 2/3$ .

acoustic (Doppler) peak in the CMB temperature power spectrum [24, 25], We pointed out above that the position of the acoustic peak as a function of multipole number (neglecting its height) is a measure of the flatness of the universe, and so supports the previous argument for negative pressure [26]. Now we point out that recent observations suggest that the amplitude of the peak is substantially higher than the value predicted for the standard cold dark matter (CDM) model [9, 27]. Various factors can account for the discrepancy: a negative pressure component, higher than anticipated baryon density, lower than anticipate Hubble parameter, and positive spectral tilt are all examples [24, 25]. Given what is already known about constraints on the baryon density and Hubble constant from other observations, a negative pressure component is the most likely explanation for the peak height. Improvements in measurements over the next few years based on long duration balloon experiments (such as *BOOMERANG*) and the MAP satellite experiment will dramatically reduce the current uncertainties. Perhaps the CMB test for a negative pressure component will be the most compelling ultimately.

*The cosmic triangle:* The observational evidence for negative pressure can be summarized visually in a “cosmic triangle” diagram [9], as described in Figure 4. The triangle is based on the Friedmann equation,

$$H^2 \equiv \left(\frac{\dot{a}}{a}\right)^2 = \frac{8\pi G}{3}\rho_m + \frac{8\pi G}{3}\rho_\Lambda - \frac{k}{a^2}, \quad (2)$$

where  $H$  is the Hubble parameter,  $\rho_m$  is the matter density,  $\rho_\Lambda$  is the vacuum density, and  $k = 0, \pm 1$  is the spatial curvature. Dividing through by  $H^2$ , one finds

$$1 = \Omega_m + \Omega_\Lambda + \Omega_k \quad (3)$$

where  $\Omega_m \equiv (8\pi G/3H^2)\rho_m$ ,  $\Omega_\Lambda \equiv (8\pi G/3H^2)\rho_\Lambda$ , and  $\Omega_k = -k/a^2H^2$ . Note that  $\Omega_k$  is defined to include the negative sign so that  $\Omega_k < 0$  for a closed universe and  $> 0$  for an open universe. The Friedmann equation has been converted to a sum rule in which  $\Omega_i$  represents the fractional contribution of component  $i$  to the expansion of the universe. Because the energy densities in the two components decrease at different rates as the universe expands, the fractional contributions may change; however, the sum rule must be obeyed at all times.

Every point in the triangle has the property that the perpendicular distances to the three edges of the triangle sum to unity; so, if the three distances correspond to the three  $\Omega_i$ , every point in the triangle obeys the sum rule. The evolution of the universe corresponds to a trajectory in the cosmic triangle plot in Figure 4. A central goal of observational cosmology is to determine the point corresponding to the present universe.

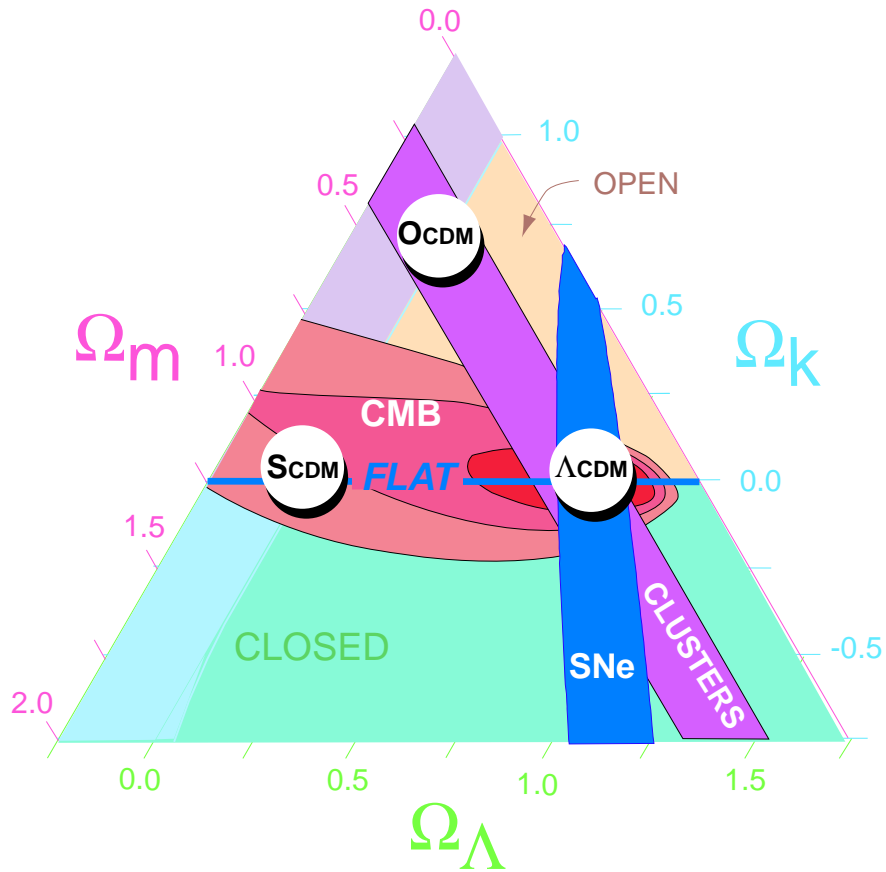


*Figure 5.* Current observational constraints are represented on the cosmic triangle plot. The tightest constraints from measurements at low red shift (clusters, including the mass-to-light method, baryon fraction, and cluster abundance evolution), intermediate red shift (supernovae), and high red shift (CMB) are shown by the three bands. The bands for cluster and supernovae measurements represent  $1\sigma$  uncertainties;  $1\sigma$ ,  $2\sigma$  and  $3\sigma$  uncertainties are shown for the CMB.

The current measurements of the CMB temperature anisotropy power spectrum are shown in Figure 2. In the plot, the CMB data is compared with the predicted power spectra for the best fit standard, open and  $\Lambda$  cold dark matter models. The data strongly favors flat models over open models and moderately favors models with  $\Lambda$  (or quintessence) over the Einstein-de Sitter model.

Figure 5 illustrates the constraints from measurements of cluster abun-

dance, supernovae, and the cosmic microwave background on the parameter-space. Because the cluster abundance, supernova and CMB are measuring conditions in the universe in different red shift regimes, the contours of maximum likelihood are oriented at different angles. As a result, the independent measurements combine to form an overconstrained region of concordance. The current concordance region is centered near the  $\Lambda$ CDM model with  $\Omega_m \approx 0.3$  and  $\Omega_\Lambda \approx 0.7$ . Figure 5 also illustrates how the cosmic acceleration of the universe can be deduced from supernovae measurements alone or, independently, from the combination of cluster abundance (which constrains the matter density) and the CMB (which constrains flatness). Because of the high acoustic peak indicated in the most recent CMB results, a likelihood analysis reveals that the CMB data alone points to the  $\Lambda$ CDM model being modestly favored compared to the standard CDM model and significantly favored compared to the open (adiabatic) model.

### 3. What are the the explanations?

The candidates for the negative pressure component are a cosmological constant [4, 19] or quintessence [1, 3]. A cosmological constant is a time-independent, spatially homogeneous component which is physically equivalent to a non-zero vacuum energy: each volume of empty space has the same energy density at each moment in time. The pressure of vacuum density equals precisely the negative of the energy density, or  $w \equiv p/\rho = -1$ . Quintessence is a time-varying, spatially inhomogeneous component with negative pressure,  $-1 < w < 0$ . Formally, vacuum energy density is quintessence in the limit  $w \rightarrow -1$ , although the two forms of energy are quite distinct physically. Quintessence is a dynamical component whereas vacuum density is inert.

The term “quintessence” was introduced historically in an attempt to resolve a different problem of acceleration. Namely, in ancient times, the centripetal acceleration of the moon was inconsistent with the ancient physical world-view. According to this view, the universe consists of four constituents: earth, air, fire and water. An important property of earth is that it is the densest and so everything made of earth falls to the center of universe (from which one concludes that the Earth is the center of the universe). The moon is problematic in that it has mountain and valley feature like the Earth, and yet the moon does not fall to the center. One proposed explanation was that there is a fifth element, or “quintessence,” which permeates space and keeps the moon suspended, but which otherwise does not interact with the other four components. Millenia later, the term is being re-introduced to resolve another problem of cosmic acceleration. Cosmological models composed of four basic elements, baryons, leptons, photons and

cold dark matter cannot explain the apparent acceleration in the universe on a grander scale, and perhaps quintessence is the cause.

The prime example of quintessence discussed in the literature [1, 3] is a scalar field  $Q$  slowly rolling down a potential  $V(Q)$ . The pressure of a scalar field is the difference between the kinetic and potential energy,  $p = \frac{1}{2}\dot{\phi}^2 - V$ . “Slow-roll,” a condition in which the kinetic energy is less than the potential energy, produces negative pressure. The notion that a scalar field can produce negative pressure and cosmic acceleration was already established with “new inflation,” [6, 7] in which the scalar inflaton field undergoes slow-roll and drives inflation. The difference is that the energy scale for quintessence is much smaller and the associated time-scale is much longer compared to inflation. Although we will consider only the scalar field example in the rest of the paper, other forms of quintessence are possible. For example, a tangled web of non-abelian cosmic strings [37, 38] produces a negative pressure with  $w = -1/3$ , and a network of domain walls has  $w = -2/3$ .

### 3.1. QUINTESSENCE: NOT A TIME-VARYING COSMOLOGICAL CONSTANT!

Quintessence is sometimes referred to as a “time-varying cosmological constant” or “smooth component,” based on its average effect on the expansion of the universe. Discussions of a time-varying cosmological constant in the smooth approximation date back at least as far as the papers by the Russian physicist, Bronstain in 1933 [39], and the idea has been revisited frequently over the intervening decades [1, 2, 3]. However, treating quintessence in this manner oversimplifies the concept to a point where some of the most difficult theoretical challenges and intriguing possibilities are lost.

A good analogy is the description of inflation as a “de Sitter phase,” a finite period in which the universe is dominated by a cosmological constant. The description captures some of the gross features of inflation, such as the superluminal expansion. Yet, a de Sitter phase of finite duration is a physical contradiction. Once one appreciates that inflation must be of finite duration, it then becomes clear that a dynamical component is required instead of a cosmological constant, and immediately issues arise: what is the nature of the dynamical component? how did inflation begin? how did it end? what happened to the energy that drove the inflationary expansion? By pursuing these issues, one encounters one of the great surprises of inflation: the existence of tiny density fluctuations following inflation as a result of the stretching of quantum fluctuations from microscopic scales to cosmic scales [40, 41, 42, 43]. One is also led to consider the associated problem of tuning required to insure that the density fluctuations have an acceptable amplitude. Describing inflation as a de Sitter phase misses these important

features.

Similarly, describing quintessence as a time-varying cosmological constant is a physical contradiction. Nor can quintessence be properly considered a smooth component. An energy component which is varying in time but spatially homogeneous contradicts the equivalence principle. See Section IIIA. The moment one realizes that full dynamics must be specified, a host of theoretical issues arise, just as in the case of inflation). This more serious treatment is only recent. The pioneering work was done by B. Ratra and J. Peebles in the late 1980's [3], and, more recently, a systematic march through these issues has appeared in a series of papers by R. Caldwell and students R. Dave, L. Wang, I. Zlatev, and G. Huey [1, 20, 44, 45, 46, 50, 51, 52, 53]. As a result of their work, many of the most worrisome aspects of quintessence are well-understood and under control.

### 3.2. SOME BASIC THEORETICAL ISSUES AND THEIR RESOLUTION

This subsection raises basic questions that arise when one considers the dynamical aspects of a quintessence component and the answers that have been found in recent studies.

*Can quintessence be perfectly smoothly distributed?* No. A time-varying but smoothly distributed component is inconsistent with the equivalence principle [1, 44, 54]. If the scalar field  $Q(\tau, x)$  is separated into spatially homogeneous and inhomogeneous pieces,  $Q(\tau, \vec{x}) = Q_o(\tau) + \delta Q(\tau, \vec{x})$ , where  $\tau$  is the conformal time, then, the Fourier transform of the fluctuating component obeys the wave equation [44]

$$\delta Q_k'' + 2aH\delta Q_k' + (k^2 + a^2V_{,QQ})\delta Q_k = -\frac{1}{2}h_k'Q_o' \quad (4)$$

where the prime denotes  $\partial/\partial\tau$ , the index  $k$  indicates the Fourier transform amplitude,  $V_{,QQ}$  is the second derivative of the quintessence potential  $V$  with respect to  $Q$ , and  $h$  is the trace of the synchronous gauge metric perturbation. Even if one sets  $\delta Q(\tau, \vec{x}) = 0$  initially,  $\delta Q(\tau, \vec{x})$  cannot remain zero if the source term on the right-hand-side is non-zero. For quintessence, the right-hand-side is non-zero because  $Q_o'$  is non-zero (the field is rolling) and, so long as one considers practical models where matter clusters,  $h_k'$  is non-zero. Hence,  $Q$  cannot remain perfectly homogeneous.

*If  $w = p/\rho < 0$ , is the sound speed imaginary? Does this mean that inhomogeneities suffer catastrophic gravitational collapse?* No. The sound speed squared is  $dp/d\rho$ , which may be positive even though  $w = p/\rho$  is negative. In many cases (including slow-rolling scalar fields), the sound speed is a function of the wavenumber,  $k$ . At small wavenumbers, corresponding to

superhorizon scales, the sound speed may be imaginary formally, but this has no physical significance since superhorizon modes do not propagate. At wavenumbers corresponding to subhorizon scales, the sound speed is real and positive [1, 44, 54]. For example, for the scalar field, the dispersion term in (4) indicates a  $k$ -dependent sound speed  $v_k^2 = (1 - a^2 V_{,QQ}/k^2)^{-1}$ . Recall that quintessence has negative pressure because  $Q$  is rolling slowly. The slow-roll means that the curvature of the potential is less than the square of the Hubble damping scale,  $H^2 > V_{,QQ}$ . For modes inside the horizon,  $k^2/a^2 > H^2$ , the sound speed is relativistic on scales much smaller than the horizon ( $v_k \rightarrow 1$ ) and becomes non-relativistic on large scales comparable to the horizon ( $v_k \rightarrow 0$ ). Formally, the sound-speed becomes imaginary on superhorizon scales, but that has no physical significance because superhorizon modes do not propagate.

*To what extent do scalar fields span the possible ways  $w$  can change as a function of red shift?* Scalar fields completely span the space of possibilities for  $w(a)$ . Given the evolution of  $w(a)$ , we may reconstruct the equivalent potential and field evolution,  $V(Q[a])$ , using the parametrized system of integral equations [35, 36]

$$V(a) = \frac{3H_0^2 \Omega_Q}{16\pi G} [1 - w(a)] \exp \left( 3 \left[ \log \frac{a_0}{a} + \int_a^{a_0} \frac{d\tilde{a}}{\tilde{a}} w(\tilde{a}) \right] \right) \quad (5)$$

$$Q(a) = \sqrt{\frac{3H_0^2 \Omega_Q}{8\pi G}} \int_{a_0}^a d\tilde{a} \frac{\sqrt{1 + w(\tilde{a})}}{\tilde{a} H(\tilde{a})} \exp \left( \frac{3}{2} \left[ \log \frac{a_0}{\tilde{a}} + \int_{\tilde{a}}^{a_0} \frac{d\hat{a}}{\hat{a}} w(\hat{a}) \right] \right) \quad (6)$$

Note that we implicitly require the Einstein-FRW equation for  $H(a)$  to evaluate  $Q(a)$ , so that the form of the potential which yields a particular equation-of-state depends on all components of the cosmological fluid, not just the quintessence. For simple  $w(a)$ , these equations can be combined to give an analytic expression for  $V(Q)$ . Otherwise,  $V(Q)$  can be computed numerically and approximated by a fit.

Hence, even if quintessence does not consist of a physical scalar field, studying scalar fields suffices to study all possible equations-of-state. The equation-of-state is sufficient to specify the background evolution. To include the perturbations due to quintessence, one also needs to determine the anisotropic stress. If quintessence is composed of strings [37, 38] or tensor fields [48], say, the anisotropic stress cannot be mimicked by a scalar field. However, the differences in the perturbative effects are typically small and so a scalar field can be used as a first approximation.

*Doesn't quintessence introduce nearly an infinite number of free parameters in the choice of  $V(Q)$ ? (If so, the concept has no useful, predictive power.)* Yes and no. The situation is very similar to inflation. Once one determines that inflation must be driven by a dynamical energy component, such as a

rolling scalar field, the concern arises that there are an infinite number of choices for the inflaton potential energy. In practice, though, there are only a few degrees of freedom relevant to observations because the observables depend only on the behavior of the inflaton over the last 60 e-folds before the end of inflation. During the last 60 e-folds, the inflaton traverses only a very small range of the potential which can be parameterized by a few degrees of freedom. Hence, in practice, inflationary predictions only depend on a small number of parameters, which is why the theory has powerful predictive power.

Similarly, observable consequences of quintessence occur between red shift  $z = 5$  and today when the  $Q$  field traverses only a small range of its potential. Thus, the possible potentials  $V(Q)$  can be effectively parameterized by only one or two constants [50]. The constants might be chosen as  $V(Q)$  and  $V'(Q)$  today. A more convenient choice is the effective ( $\Omega_Q$ -weighted) equation of state

$$\bar{w} \equiv \int \Omega_Q(a)w(a)da / \int \Omega_Q(a)da, \quad (7)$$

and the effective first time-derivative  $\dot{w}$ ,

$$\dot{\bar{w}} \equiv \int dz \Omega_Q(z)[\dot{w}]^2 / \int dz \Omega_Q(z) \quad (8)$$

where  $\dot{w} \equiv dw/d\ln z$ . Most observations are only sensitive to  $\bar{w}$  and, in some cases,  $\dot{\bar{w}}$ .

*Does quintessence require a small mass parameter?* No. Consider the simple case of inverse power-law potentials:  $V(Q) = M^{4+\alpha}/Q^\alpha$ . Quintessence overtakes the matter density and induces acceleration when  $Q \approx M_p$ , where  $M_p$  is the Planck scale. To have  $\Omega_Q \approx 0.7$  today requires  $V(Q \approx M_p) \approx \rho_m$ , where  $\rho_m \approx 10^{-47} \text{ GeV}^4$  is the current matter density; this imposes the constraint  $M \approx (\rho_m M_p^\alpha)^{1/(\alpha+4)}$ . For low values of  $\alpha$  (or for the exponential potential), this forces  $M$  to be a tiny mass, as low as 1 meV for the exponential case. However, we note that  $M > 1 \text{ GeV}$  — comparable to particle physics scales — is possible for  $\alpha \geq 2$ . Hence, our solution to the missing energy problem does not require the introduction of a new mass hierarchy in fundamental parameters. It is the case that  $V$  must be of order  $(1 \text{ meV})^4$ , and  $V''$  must be of order  $H^2 \approx (10^{-42} \text{ GeV})^2$ . But the example shows that these values can be achieved without invoking a tiny mass parameter [51].

*To what extent must the analysis of observations be modified because quintessence is spatially inhomogeneous?* Conventional treatments of the mass power spectrum and the CMB temperature rely on the mass density being the only spatially inhomogeneous component. The Press-Shechter formalism



[46], the computation of the linear mass power spectrum [1, 44], the non-linear corrections [47], and the CMB temperature power spectrum [1, 44] all must be modified to properly incorporate the spatial inhomogeneities in quintessence. In the typical case, the modification is a small, quantitative correction. In extreme cases, the spatial inhomogeneities can produce anomalous bumps in  $P(k)$  (not unlike the bumps reported in some large-scale structure surveys) and amplify peaks in the CMB power spectrum (not unlike some recent observations) [49].

*Isn't quintessential cosmology sensitive to initial conditions for  $Q$  and  $\dot{Q}$  as well as to the potential parameters?* It depends. For many potentials discussed in the literature [1, 3], the initial value of  $Q$  and  $\dot{Q}$  must be finely tuned to obtain the correct value of  $\Omega_Q$  today. The tuning of the initial field expectation value is required in addition to tuning the potential parameters. Since the initial conditions for the field are hard to control, the scenario seems even more contrived than the tuning of the cosmological constant. However, as discussed in the next subsection, a large class of potentials has been found for which the cosmology is insensitive to the initial  $Q$  and  $\dot{Q}$  because there exist classical attractor solutions to the equations-of-motion which result in the same value of  $\Omega_Q$  independent of the initial conditions [51, 52, 55].

*Isn't quintessential cosmology sensitive to the initial conditions for  $\delta Q$ , the spatial fluctuations in  $Q$ ?* No. Without the source term in Eq. (4), perturbations in  $Q$  would remain small due to the highly relativistic nature of  $Q$ . With the source term, the fluctuations in  $Q$  do grow significantly at a rate determined by fluctuations in the metric which, in turn, are determined by the clustering matter component [1, 44, 54]. The amplitude of the perturbation as it enters the horizon depends principally on the source term and is insensitive to the initial conditions in  $Q$  itself. In particular, the numerical difference in predictions obtained assuming adiabatic initial conditions for  $\delta Q$  (as might be expected after inflation) versus smooth initial conditions is negligible [36].

Taken together, the answers to these questions go a long way to transforming quintessence from a seemingly arbitrary proposal with many free parameters and choices of initial conditions to a predictive scenario described by few parameters. What remains to be resolved is the cosmic coincidence problem.

### 3.3. THE COSMIC COINCIDENCE PROBLEM

The key problem posed by a negative pressure component and, in my view, the principle motivation for considering quintessence is the cosmic coincidence problem. The problem has two aspects whose resolution may require

two different concepts. One puzzle is to explain why the energy density of the negative pressure component,  $\rho_Q \sim (1 \text{ meV})^4$ , is so tiny compared to typical particle physics scales. At present, some discount the current evidence for negative pressure simply because it requires a seemingly extraordinary fine-tuning. However, if the evidence described in Part II progresses and becomes overwhelmingly decisive in the next few years, which is technologically feasible, then the view will change. Instead of the small energy density being a problem for cosmology, it will become a new, fundamental parameter whose measured value must be explained by particle physics, just as particle physics is expected to explain ultimately the mass of the electron. This paper anticipates that day.

However, explaining the small value of the energy density is not enough. A second puzzle is to explain why the matter density and the energy density of the negative pressure component are comparable today. Throughout the history of the universe, the two densities decrease at different rates, so it appears that the initial conditions in the early universe have to be set with exponentially sensitive precision to arrange comparable energy densities today. For example, after inflation, the ratio of vacuum density to matter-radiation density would have to be tuned to be of order  $10^{-100}$ . Since the ratio is inferred on the basis of extrapolating a cosmological model backwards in time, the solution to the initial conditions problem may lie in the domain of cosmology, rather than particle physics. That is, perhaps the tuning may be avoided perhaps by changing the cosmological model.

What would be ideal is an energy component that is initially comparable to the matter and radiation density, remains comparable during most of the history of the universe, and then jumps ahead late in the universe to initiate a period of cosmic acceleration. This is quite unlike a cosmological constant. However, recently, a large class of quintessence models with “runaway scalar fields” have been identified which have many of the desired properties.

### 3.4. RUNAWAY SCALAR FIELDS AND THE STICKING POINT THEOREM

Runaway scalar fields are promising candidates for quintessence. We use the term “runaway scalar fields” [56] to refer to cases in which the potential  $V(Q)$ , the slope  $V'(Q)$ , the curvature  $V''(Q)$ , and the ratios,  $V'/V$  and  $V''/V$  all converge to zero as  $Q \rightarrow \infty$ . The potentials occur in string and M-theory models associated with the many moduli fields or with fermion condensates [57, 58, 59, 60, 61, 62]. The potentials are typically flat to perturbative order but have runaway potentials when non-perturbative effects are included. Inverse power-law potentials, general functionals with inverse powers or fractional powers of the field (or condensate) are examples of runaway potentials.

A runaway field has a simple but profound effect on cosmology. The ultimate fate of the universe is sealed: the universe is destined to undergo cosmic acceleration [56]. The prediction is as sure as if one had introduced a positive cosmological constant into the theory. The argument is based on a simple theorem we refer to as the “sticking point theorem”: Given a runaway potential  $V(Q)$ , there is a smallest value of the field  $Q_{sp}$  for which  $V'(Q_{sp})/V(Q_{sp}) < 8\pi Q_{sp}/M_p^2$  and  $V''(Q_{sp})/V(Q_{sp}) < 8\pi G/3$ ; that is, since  $V'/V$  and  $V''/V$  converge to zero at large  $Q$ , there must be a smallest value  $Q_{sp}$  such that the ratios satisfy these two inequalities for all  $Q \geq Q_{sp}$ . (One could imagine potentials where all  $Q$  satisfy the inequalities. Then, the sticking point theorem is trivially satisfied; see below.)

The sticking point theorem says that, for all  $Q > Q_{sp}$ , the rolling field is critically damped by the Hubble expansion and the field is frozen. The word “frozen” is used judiciously – one should imagine a frozen glacier which slowly flows downhill. In this case, the field flows so slowly downhill that the energy density decreases much more slowly than matter and radiation density. The field energy eventually overtakes the matter and radiation, driving the universe into cosmic acceleration.

The proof is trivial: For any  $Q > Q_{sp}$ , it must be that  $V''(Q)/V(Q) < 8\pi G/3$ , by the definition of  $Q_{sp}$ . Then, we have

$$V''(Q) < \frac{8\pi G}{3}V(Q) < \frac{8\pi G}{3}[\rho_{m,r} + \frac{1}{2}\dot{Q}^2 + V(Q)] = H^2, \quad (9)$$

where  $\rho_{m,r}$  is the background matter-radiation density, which is positive. The right hand equation is the definition of the Hubble parameter according to the Friedmann equation. The chain of relations reduces to  $V'' < H^2$ , which is precisely the condition for the  $Q$ -field kinetic energy density to be overdamped by the Hubble expansion (assuming the slope,  $V'$ , is negligible) so as to force slow-roll and negative pressure [7]. The condition on  $V'/V$  is the condition that the slope be negligible. Hence, the sticking point theorem assures that, once the field rolls past the sticking point,  $Q$  slows to a crawl and acts as a negative pressure component. Since the potential is decreasing, there is nothing to stop  $Q$  from ultimately reaching and surpassing the sticking point. Beyond the sticking point, the potential energy of the  $Q$ -field is sufficient to create a Hubble damping that freezes the field, independent of the value of the matter and radiation density. It is just a matter of time before this energy density comes to dominate the universe. The corollary is that it is just a matter of time before the energy density of the runaway field overtakes the matter and radiation, and cosmic acceleration commences. For most runaway potentials, the sticking point corresponds to a large expectation value of the field and a small energy. This feature of runaway fields satisfies in a very rough, qualitative way the

condition desired to explain why cosmic acceleration begins late in the history of the universe when the mean density is small. There remains the issue of why acceleration commences after 10 billion years rather than 10 million years or 10 trillion years, but the qualitative character of runaway fields seems, at least to this author, to be an attractive feature which may well be incorporated in the final answer.

### 3.5. TRACKER FIELDS AND TRACKING POTENTIALS

There are different ways the runaway field may come to surpass the sticking point, which leads to different cosmological scenarios. We discuss two examples: tracker models and creeper models.

Tracker fields [51, 52] are runaway fields in which the equation-of-motion has an attractor-like solution so that the evolution of  $Q$  is insensitive to the initial conditions for  $Q$  and  $\dot{Q}$ . In order to have an attractor solution, one requirement is that  $\Gamma \equiv V''V/(V')^2$  exceed  $5/6$  and be nearly constant [52]. The only constraint on the initial energy density in the tracker field is that it be less than or equal to the initial matter-radiation energy and greater than the present-day matter density. (As we shall see, this condition is necessary in order for  $Q$  to converge to the attractor solution before the present epoch.) This constraint allows an extraordinary range of initial conditions for  $\rho_Q$  spanning over 100 orders of magnituder. The range includes the physically well-motivated possibility of equipartition between quintessence and matter-radiation. The term "tracker" refers to the fact that the cosmology follows the same evolutionary track independent of initial conditions. See Figure 6.

The attractor solution has the property that, beginning from the initial  $Q$  and  $\dot{Q}$ ,  $Q$  rapidly converges to the point on the potential where  $V'' \approx H^2$ . The Hubble parameter  $H$  is determined by the matter and radiation density. As the universe expands and  $H$  decreases,  $Q$  moves down the potential so as to maintain the condition  $V'' \approx H^2$ . In this sense, the evolution of the  $Q$ -field controlled by the matter-radiation density rather than evolving independently according to its own potential. This is the distinctive feature of tracker fields. The controlled evolution continues until  $Q$  finally surpasses the sticking point. Then, its own potential energy density is sufficient to freeze the field and cause it to overtake the background energy.

What if the initial energy density is far below the value where  $V'' = H^2$  but  $Q < Q_{sp}$ ? We refer to this as the "undershoot" initial condition. Since  $V''/V$  is decreasing, lower energy density means that the initial  $V''$  must be much less than  $H^2$ . The evolution of  $Q$  is overdamped by the Hubble expansion, and so its value remains nearly constant. The field has not surpassed the sticking point ( $Q < Q_{sp}$ ), and the field is only frozen

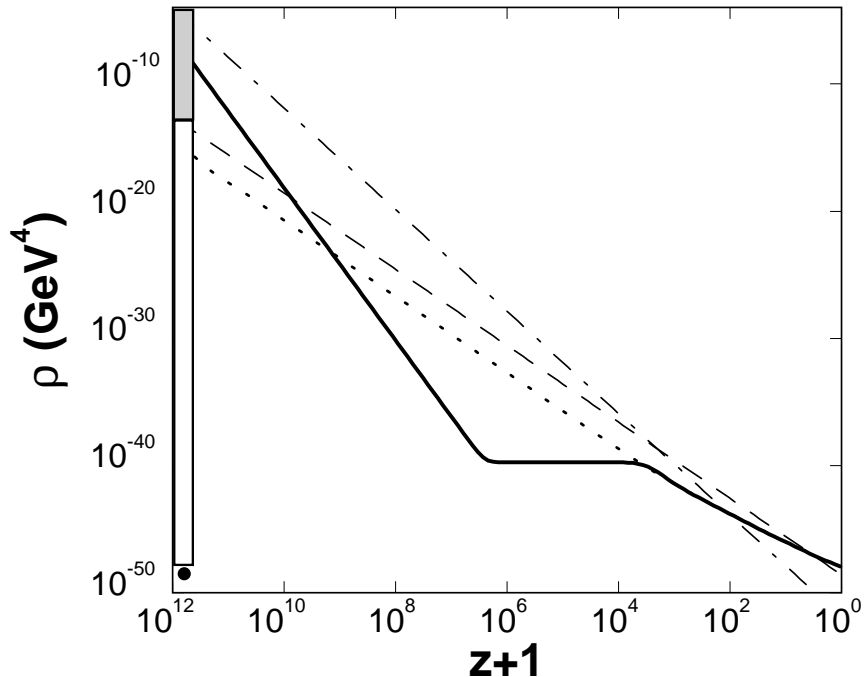


*Figure 6.* Energy density versus red shift for the evolution of a tracker field. For computational convenience,  $z = 10^{12}$  has been arbitrarily chosen as the initial time when the field begins to roll. The white and grey bars represent the span of allowed initial conditions for  $\rho_Q$  (which corresponds to 100 orders of magnitude if extrapolated back to inflation). The white bar on left represents the undershoot type of initial condition and the grey bar represents the overshoot. The solid black circle represents the unique initial condition required if the missing energy consists of vacuum energy density. The dotted curve is the attractor (tracker) solution. The solid thick curve illustrates the evolution beginning from an overshoot initial condition in which  $\rho_Q$  has a value greater than the tracker solution.  $Q$  rushes rapidly down the potential, overshooting the tracker solution and the matter density, and freezes. As the universe expands,  $H$  decreases to a point where  $V'' \approx H^2$  and the field joins the tracker solution.

because of the matter-radiation density contribution to  $H$ . As the universe expands, the matter-radiation density eventually decreases to a point where  $V'' \approx H^2$  and the field becomes unfrozen. The field begins to roll down the potential with  $V''$  tracking  $H^2$  just as it would if the field had begun on the attractor solution initially. Ultimately,  $Q$  passes the sticking point and cosmic acceleration begins.

What if the initial energy density begins above the value where  $V'' = H^2$  (the “overshoot” initial condition)? See Figure 6. In this case,  $V'' \gg H^2$  and the Hubble damping is irrelevant at first. The potential is so steep that the field rapidly accelerates to a condition where its energy density is

dominated by its kinetic energy. A field dominated by kinetic energy has  $w = 1$  and decreases as  $1/a^6$ . The field energy rapidly falls compared to the matter and radiation at such a rate that it overshoots and falls below the attractor solution,  $V'' \approx H^2$ . Eventually, though, the Hubble damping red shifts away the kinetic energy and the field becomes frozen after a displacement of [51, 52]:

$$\Delta Q \approx \left( \frac{3}{4\pi} \Omega_{Qi} \right)^{1/2} M_p, \quad (10)$$

where  $\Omega_{Qi}$  is the initial ratio of  $\rho_Q$  to the critical density and  $M_p$  is the Planck mass. (Typically, the initial value of  $Q$  is negligible, so  $Q \approx \Delta Q$  when the field is frozen.) Now the field is frozen at a point where  $V'' \ll H^2$ , the initial condition of the undershoot case. The frozen values of  $Q \approx \Delta Q$  and  $V''$  are independent of the potential (since the kinetic energy dominates during the as  $Q$  rapidly falls), but they are dependent on the initial value of  $\rho_Q$ , as shown in Eq. (10) above. Nevertheless, this is irrelevant for cosmology since the energy density in  $Q$  is much smaller than matter and radiation density during the frozen period. As in the undershoot case, the field remains frozen until  $H^2$  decreases to a point where it matches  $V''$  and the field joins the tracker solution. By the time  $\rho_Q$  grows to influence cosmology,  $Q$  is on the same evolutionary track as if  $Q$  and  $\dot{Q}$  had begun on the tracker solution in the first place.

The tracker solutions lead to a new prediction: a relationship between  $\Omega_m$  and the equation-of-state for  $Q$ ,  $w_Q$  [51, 52]. The relationship occurs because, for any given potential, the attractor solution is controlled by only one free parameter, which can be chosen to be the value of  $\Omega_m$  today (assuming a flat universe). Consequently, once the potential and  $\Omega_m$  are fixed, no freedom remains to choose independently the value of  $w_Q$  today. There is some variation from potential form to potential form; see Figure 7. But, the variation is limited and, most importantly, includes a forbidden region between  $w_Q = -1$  and  $w_Q \approx -3/4$ .

To construct models with  $w_Q$  between  $-1$  and  $-3/4$ , one has to consider rather poorly motivated and fine-tuned potentials. An example is  $V(Q) \sim 1/Q^\alpha$  where  $\alpha \ll 0.1$  is tuned to be a tiny fractional power so that  $V(Q)$  is designed to be nearly like a cosmological constant. Adding a true cosmological constant to  $V(Q)$  would also allow  $w_Q \rightarrow -1$ , but then there is no point to having the tracker field. The  $\Omega_Q$ - $w_Q$  relation we present is intended as a prediction that distinguishes cases where there is no true cosmological constant from cases where there is.

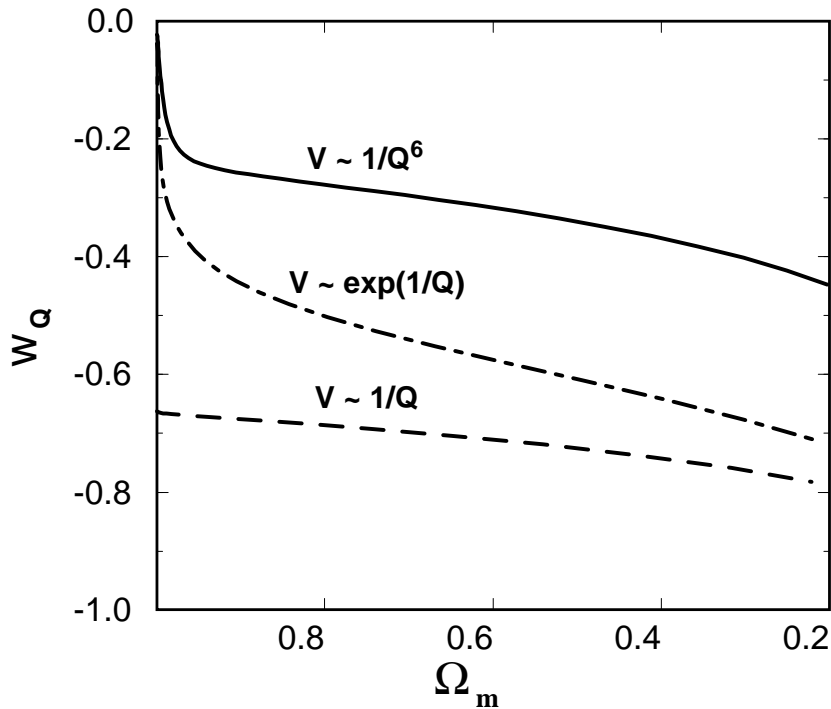


Figure 7. The  $\Omega_Q$ - $w_Q$  relation can be illustrated on a plot of  $w_Q$  versus  $\Omega_m = 1 - \Omega_Q$ . The predictions are shown for various potentials. Note that the forbidden region at values of  $w_Q$  less than  $-0.75$ .

### 3.6. CREEPING QUINTESSENCE

An alternative possibility, “creeping quintessence,” [56] occurs for the very same tracker potentials if the initial energy density in the  $Q$ -field greatly exceeds the matter-radiation density. Then, as in the overshoot case discussed in the previous subsection, the field begins with  $V'' \gg H^2$  and rapidly accelerates down the potential until the kinetic energy dominates the potential energy. As before, the field kinetic energy red shifts away as  $Q$  rolls a distance [52, 56]:

$$\Delta Q = \sqrt{\frac{3}{4\pi}} \left( 1 + \frac{1}{2} \ln \left( \frac{\rho_{Qi}}{\rho_{Bi}} \right) M_p \right). \quad (11)$$

Note that this expression is different from Eq. (10) because here  $\rho_{Qi} > \rho_{Bi}$ , where  $\rho_{Bi}$  is the initial background matter-radiation density, and the field rolls farther than overshoot case for the tracker field. The  $Q$ -field rolls so far that it overshoots not only the initial matter density, but also the sticking

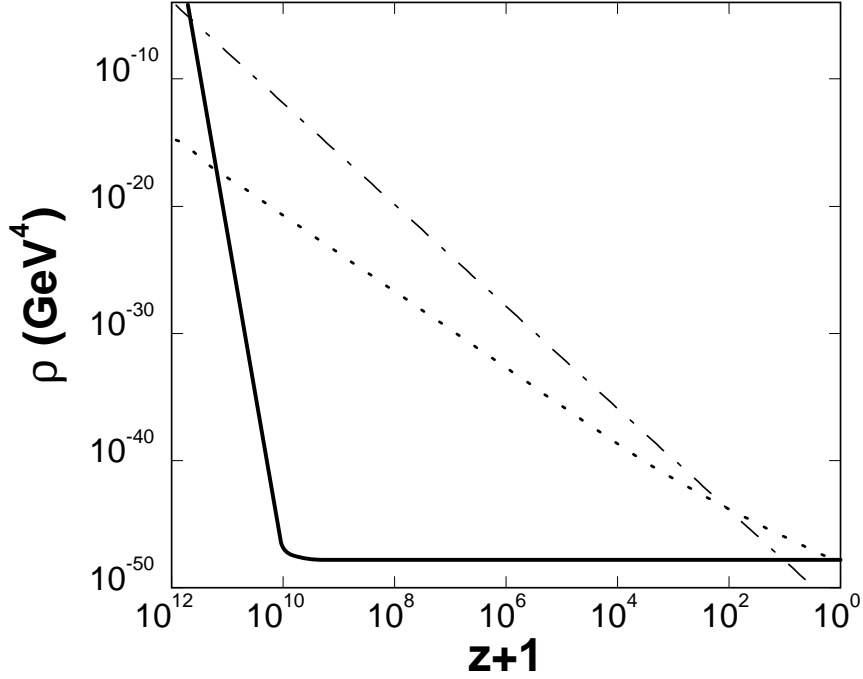


*Figure 8.* A plot showing the case for creeping quintessence in which the field overshoots the sticking point and freezes early in the history of the universe. Compare to Figure 6, in which the energy density eventually joins a tracker solution. Here, once frozen, the field rolls very slowly for the rest of the history of the universe. Consequently,  $w$  is very close to  $-1$ .

point before it finally freezes. See Figure 8. Now, the field is frozen and remains frozen forever, never joining the tracker solution. Because the field overshoots the sticking point by a significant margin, the energy density is tiny compared to the matter-radiation density, and equation of state is  $w \approx -1$ . The field creeps down the potential for the remainder of the history of the universe, with  $\rho_Q$  eventually overtaking the matter-radiation energy density and inducing cosmic acceleration.

The creeping case differs in several ways from the tracker potential. First, the creeping scenario is possible for a somewhat wider range of potentials. Since it never utilizes the tracker features, the condition on  $\Gamma$  can be dropped. All that is required is a sticking point at sufficiently low energy. Second, the scenario is more sensitive to initial conditions because the value of  $\rho_Q$  at which  $Q$  freezes is dependent on the degree to which the field overdominates the background density. However, one observes from Eq. (11) that the value at which  $Q$  freezes depends only logarithmically on



$\rho_{Qi}/\rho_{Bi}$ , which seems to be a relatively mild sensitivity to initial conditions [56].

The disadvantage of creeping quintessence is that  $w$  is very close to  $-1$  today so that distinguishing it from a vacuum density is difficult. There is no significant difference in terms of cosmic evolution, astrophysics, or the cosmic microwave background. In most quantum field theories,  $Q$  couples through quantum corrections to other interactions, and time-variation in  $Q$  results in time-varying constants. Here, the field is moving so slowly that any variation in coupling constants is exponentially small! In addition to cosmic acceleration, the ultra-slow evolution of couplings constants is an intriguing consequence of this scenario that would be very difficult to detect directly.

### 3.7. WHY IS QUINTESSENCE BEGINNING TO DOMINATE TODAY?

We have argued that tracker models and, with somewhat less precision, creeper models produce nearly the same cosmic evolutionary track independent of the initial conditions for  $Q$ . This is one of the properties desired to address the cosmic coincidence problem. What remains is to determine why the track turns out to be one where  $Q$  has begun to dominate recently. The time when  $Q$  overtakes the matter density is determined by  $M$  for a quintessence potential  $V(Q) = M^4 f(Q/M)$ . The tuning of  $M$  might be viewed as similar to the tuning of  $\Lambda$  in the case of a cosmological constant.

However, there is more to the issue because different forms of  $f(Q/M)$  produce different families of tracker solutions which overtake the matter density at different times. To consider this issue, we want to change our point-of-view. Up to this point, we have imagined fixing  $M$  so that  $\Omega_Q = 1 - \Omega_m$  has the measured value today. This amounts to considering one tracker solution for each  $V(Q)$ . Now we want to consider the entire family of tracker solutions (as a function of  $M$ ) for each potential form  $f(Q/M)$  and consider whether  $\Omega_Q$  is more likely to dominate late in the universe for one one family of solutions or another.

In general,  $\Omega_Q$  is proportional to  $a^{3(w_B - w_Q)} \propto t^{2(w_B - w_Q)/(1 + w_B)}$ , where [51]

$$w_B - w_Q = \frac{2(\Gamma - 1)(w_B + 1)}{1 + 2(\Gamma - 1)}. \quad (12)$$

Hence, we find  $\Omega_Q \propto t^P$  where

$$P = \frac{4(\Gamma - 1)}{1 + 2(\Gamma - 1)}. \quad (13)$$

For two special cases ( $V \sim 1/Q^\alpha$  and  $V \sim \exp(\beta Q)$ ),  $\Gamma - 1$  is nearly constant, and, hence,  $P$  is nearly constant as well. The interpretation is

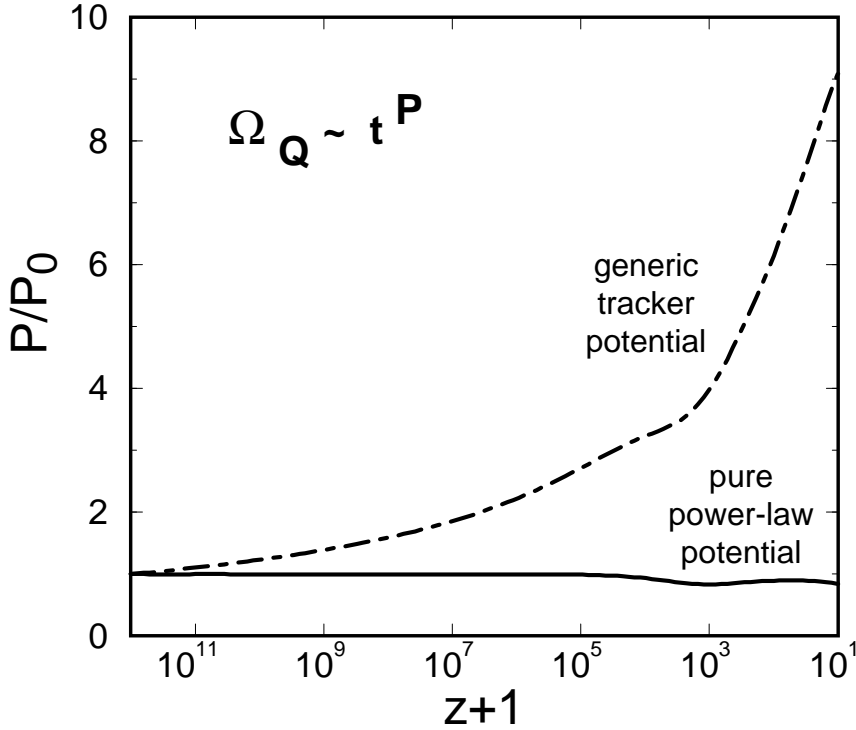
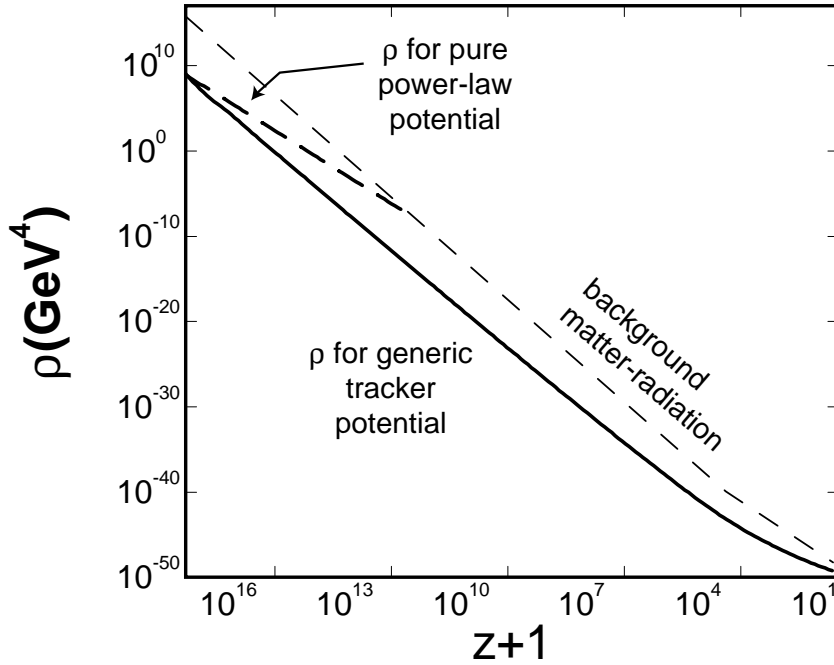


Figure 9. A plot of  $P/P_0$  versus  $t$ , where  $\Omega_Q \propto t^P$  and  $P_0$  is the initial value of  $P$ . The plot compares pure inverse power-law ( $V \sim 1/Q^\alpha$ ) potentials for which  $P$  is constant with a generic potential (e.g.,  $V \sim \exp(1/Q)$ ) for which  $P$  increases with time.

that  $\Omega_Q$  grows as the same function of time throughout the radiation- and matter-dominated epochs. So, there is no tendency for  $\Omega_Q$  to grow slowly at first and then speed up later. See Figure 9. The same situation occurs for  $\Omega_\Lambda$  for models with a cosmological constant.

However, for more general quintessence potentials,  $P$  increases as the universe ages. Consider first a potential which is the sum of two inverse power-law terms with exponents  $\alpha_1 < \alpha_2$ . The term with the larger power is dominant at early times when  $Q$  is small, but the term with the smaller power dominates at late times as  $Q$  rolls downhill and obtains a larger value. Hence, the effective value of  $\alpha$  decreases and  $\Gamma - 1 \propto 1/\alpha$  increases; the result is that  $P$  increases at late times. For more general potentials, such as  $V \sim \exp(1/Q)$ , the effective value of  $\alpha$  decreases continuously and  $P$  increases with time. Figure 9 illustrates the comparison in the growth of  $P$ .

How does this relate to why  $\Omega_Q$  dominates late in the universe? Because



*Figure 10.* A plot comparing two tracker solutions for the special case of a pure power-law ( $V \sim 1/Q^6$ ) potential (solid line) and a general potential composed of a combination of inverse power-law contributions ( $V \sim \exp(1/Q)$ ) (dot-dash). The dashed line is the background density. The two tracker solutions were chosen to have the same energy density initially. The tracker solution for the generic example ( $V \sim \exp(1/Q)$ ) reaches the background density much later than for the pure inverse-power law potential. By this measure,  $\Omega_Q$  is more likely to dominate late in the history of the universe in the generic case than for a pure power-law potential.

an increasing  $P$  means that  $\Omega_Q$  grows more rapidly as the universe ages. Figure 10 compares a tracker solution for a pure inverse power-law potential ( $V \sim 1/Q^6$ ) model with a tracker solution for a generic potential with a combination of inverse powers (in this case,  $V \sim \exp(1/Q)$ ), where the two solutions have been chosen to begin at the same value of  $\Omega_Q$ . (The start time has been chosen arbitrarily at  $z = 10^{17}$  for the purposes of this illustration.) Following each curve to the right, there is a dramatic (10 orders of magnitude) difference between the time when the first solution (solid line) meets the background density versus the second solution (dot-dashed line). Beginning from the same  $\Omega_Q$ , the first tracker solution dominates well before matter-radiation equality and the second (generic) example dominates well after matter-domination.

Hence, an intriguing conclusion is that the generic quintessence potential

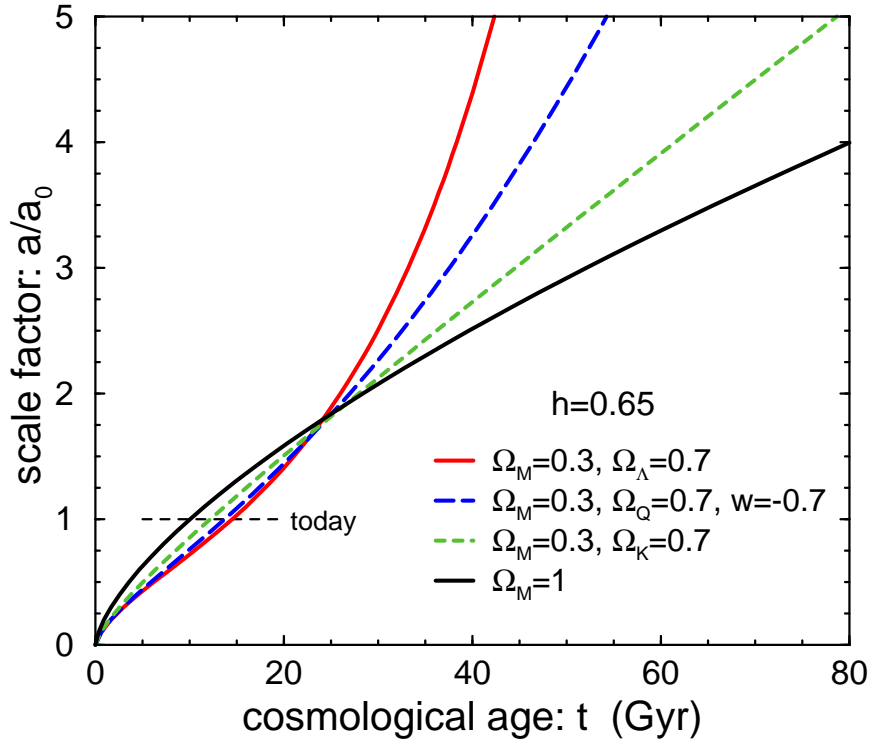


*Figure 11.* The scale factor vs. time for an Einstein-de Sitter model ( $\Omega_m = 1$ ) and three models with  $\Omega_m = 0.3$ : an open model, a flat model with quintessence ( $w = -0.7$ ), and a flat model with a cosmological constant.

has a family of solutions in which  $\Omega_Q$  tends to dominate late in the history of the universe and induces a recent period of accelerated expansion. Although the trend towards late domination is an improvement over models with cosmological constant or pure power-law or exponential  $V(Q)$ , we have not answered the quantitative question: why is  $Q$  dominating after 15 billion year and not, say, 1.5 billion years or 150 billion years. Yet further ideas are required.

#### 4. Current constraints and future tests

The observable consequences of quintessence are due to its effect on the expansion of the universe and its inhomogeneous spatial distribution. Figure 11 compares the expansion rate of universe for an Einstein-de Sitter model ( $\Omega_m = 1$ ) with three models with  $\Omega_m = 0.3$ : an open model, a flat model with quintessence ( $w = -0.7$ ), and a flat model with a cosmologi-

cal constant. The expansion rate is decelerating for the Einstein-de Sitter and open models and accelerating for the models with cosmological constant and quintessence. For a given  $\Omega_Q$ , the cosmological constant has more negative pressure and, hence, induces a greater acceleration. The present epoch corresponds to scale factor  $a/a_0 = 1$ . The figure shows that the age of the universe increases with acceleration. The open model and the models with quintessence or cosmological constant predict ages consistent with estimates based on the ages of globular clusters [21, 22].

Because the spatial inhomogeneities in the quintessence typically have small amplitudes compared to the density perturbations, they are difficult to detect. The largest effect is on the CMB anisotropy and the mass power spectrum on large scales, which is incorporated in computations of the power spectra for quintessence models [1]. Figure 12 shows the predictions for the CMB temperature anisotropy power spectrum for a series of quintessence models with different choices of  $w$ ,  $\Omega_m$  and the spectral index,  $n$ , of the primordial density fluctuation distribution. The results are compared to an Einstein-de Sitter model and a model with cosmological constant. As with a cosmological constant, quintessence increases the height of the first acoustic peak compared to the Einstein-de Sitter model. The differences in height are due to a combination of differences in equation-of-state, tilt, and normalization. Note the tiny difference in the shape of the CMB power spectra at small  $\ell$  for the quintessence models compared to the  $\Lambda$ CDM model. The effect is primarily due to the spatial inhomogeneities in the quintessence field [1, 36], as well as differences in the integrated Sachs-Wolfe contribution. Although the spatial fluctuations in the quintessence field make a large contribution to the CMB anisotropy at small  $\ell$ , the difference in the CMB power spectrum shape is nearly impossible to detect. The quintessence fluctuations become important, though, when the amplitude of the CMB anisotropy is correlated with the amplitude of the mass density fluctuations on large scales. Consider a quintessence model and a  $\Lambda$ CDM with nearly indistinguishable CMB anisotropy power spectra. The two models have nearly the same CMB anisotropy on large scales, but, for one model, spatial fluctuations in the quintessence makes a significant contribution. Consequently, the contribution of mass fluctuations is different for the two models. By measuring the mass power spectrum directly and comparing to the two model predictions, the presence or absence of spatial fluctuations in the quintessence field can be determined.

Since spatial inhomogeneities contribute significantly to the anisotropy for the quintessence case but there is no analogue for  $\Lambda$ CDM case, the fraction of the anisotropy due to mass fluctuations is different. A quintessence model and a  $\Lambda$ CDM with nearly indistinguishable CMB power spectra will predict a mass power spectrum normalization that can differ by a factor

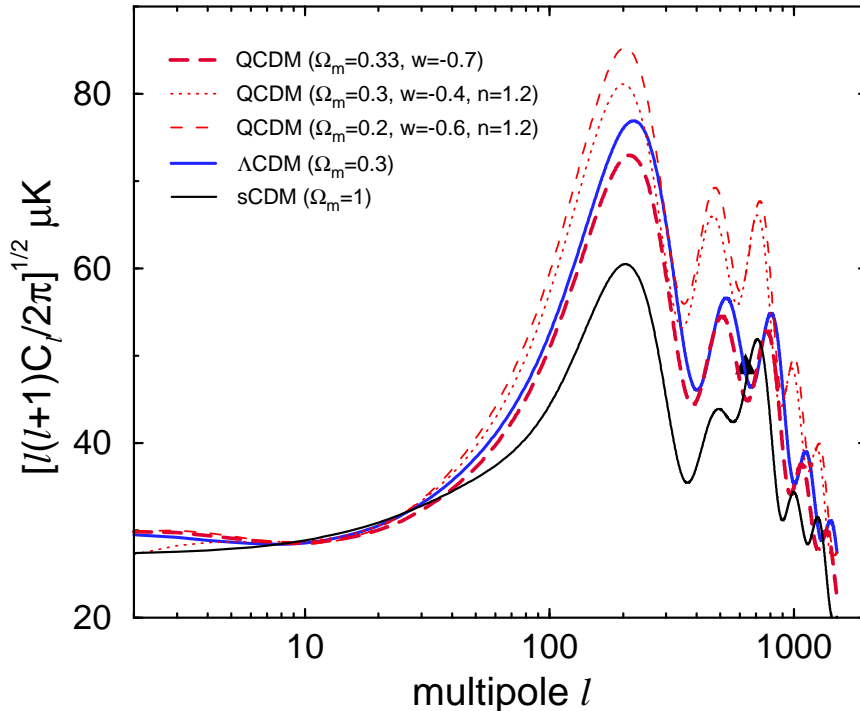
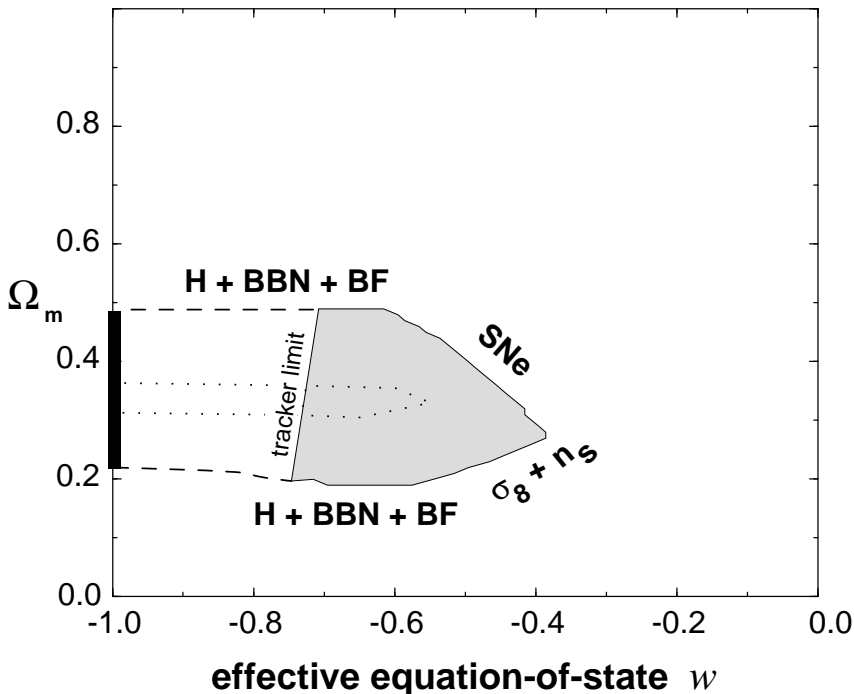


Figure 12. The CMB power spectrum for an Einstein-de Sitter model ( $\Omega_m = 1$ ), a flat model with cosmological constant ( $\Lambda$ CDM), and a sequence of flat models with quintessence (QCDM). The  $\Lambda$ CDM and QCDM models are consistent all current cosmological observations.

of two or more. Hence, correlating measurements of the CMB power spectrum and the mass power spectrum is the optimal approach for detecting the effect of spatial inhomogeneities in the quintessence field.

Based on these effects, Wang *et al.* [20] have completed a comprehensive survey of cosmological tests of quintessence models which shows that a substantial range of  $\Omega_m$  and  $w$  is consistent with current observations. The allowed region in the  $\Omega_m$ - $w$  plane is shown in Figure 13. For a given combination of  $\Omega_m$  and  $w$  to be included, there must exist a choice of the Hubble parameter, spectral tilt, and baryon density such that the model satisfies all current tests at the  $2\text{-}\sigma$  level or better. (See the original paper for a full discussion and an alternative plot using conventional likelihood analysis which shows similar results.)

In the future, it should be possible to distinguish the  $\Lambda$  or creper regime from the tracker regime with improved CMB anisotropy measurements combined with other cosmological observations [50]. The wider the difference between the actual  $w$  and  $-1$ , the easier it is to distinguish  $Q$



*Figure 13.* The region of the  $\Omega_m$ - $w$  plane consistent with current observations and theoretical constraints. The black strip on left corresponds to the allowed range for models with a cosmological constant or creeping quintessence. The grey region on right corresponds to tracker models. The gap spanning  $-1.0 < w < -0.75$  is allowed observationally, but does not fit within the tracker or creeper scenarios. (This range appears to require fine-tuning of initial conditions or more exotic potentials.) The dotted region is the 1-sigma best-fit according to maximum likelihood analysis. The markings around the allowed region indicate the measurements which delimit each boundary: Hubble constant (H), big bang nucleosynthesis (BBN), baryon fraction (BF), supernovae searches (SNe), cluster abundance ( $\sigma_8$ ), power spectrum tilt ( $n_s$ ).

from  $\Lambda$ . Measurements of the CMB power spectrum constrain models to a degeneracy curve in the  $\Omega_m$ - $w$  plane; along the degeneracy curve, changes in  $\Omega_m$ ,  $w$  and  $h$  combine to make the power spectrum indistinguishable [50]. The effects of gravitational lensing on the CMB, which may be detectable by measuring the spectrum at very small angles, reduce but do not totally eliminate the degeneracy [50]. Measurements of the Hubble parameter, deceleration parameter, or matter density can break the degeneracy, as can, perhaps, measurements of gravitational lensing arcs or improved luminosity-red shift measurements for supernovae [50, 63, 64, 65, 66]. Davis

has suggested a more direct approach in which measuring velocity dispersion (line-widths) of clusters as function of red shift is used as a cosmic barometer.

## 5. Theoretical Challenges

The quintessence scenario has progressed from a somewhat arbitrary and ill-defined concept with many free parameters to a well-defined and predictive proposal. Some of the key results have been:

- strong evidence for cosmic acceleration is found in measurements of the luminosity-red shift relation for Type IA supernovae and in the CMB temperature anisotropy (Section 2);
- in order to form large-scale structure from primordial, adiabatic density fluctuations, a negative pressure component of dark energy is required if the universe is flat and the matter density is significantly less than the critical density, as present observations indicate (Section 2);
- quintessence is stable against gravitational instability even though it has negative pressure (Section 3.2);
- quintessence models have predictive power because all observational predictions are dependent principally on two parameters, the  $\Omega_Q$ -weighted average of the equation-of-state,  $\bar{w}$  and its time derivative (Eq. 7) (Section 3.2);
- a large class of models described by “runaway potentials” lead inevitably to cosmic acceleration late in the history of the universe (*i.e.*, well below the Planck scale) (Section 3.4);
- there exists a class of “tracker potentials,” which includes a large subclass of runaway potentials, with an attractor solution such that the cosmic evolution is insensitive to initial conditions (Section 3.5);
- tracker models predict a relation between  $\Omega_m$  and  $w$  today which is distinguishable from the prediction for a cosmological constant;
- another class, “creeper potentials,” does not utilize attractor solutions but the cosmic evolution is nevertheless only mildly (logarithmically) dependent on initial conditions (Section 3.6);
- for creeper potentials,  $w$  is nearly  $-1$  today, which is impossible to distinguish from a cosmological constant using cosmological observations;
- current observations are in complete concordance with a substantial range of quintessence models, including tracker and creeper models, as well as models with a cosmological constant (Section 4).

Runaway fields and tracker/creeper potentials appear to be endemic to many unified theories, including string theory and M-theory. Furthermore, in the brane-world picture with matter-fields confined to 4-d domain walls and with gravitational interactions across the bulk, it is difficult to arrange



a constant energy density in low-energy, 4-d effective theory. In the 5-d or higher dimensional theory, a small vacuum energy on any one brane or in the bulk separating branes induces an expansion of extra-dimensions. The extra-dimensional radius or length is a scalar field in the low-energy, 4-d effective theory. From the point-of-view of the 4-d theory, the expansion of the extra dimensions appears as a change in the expectation value of the field so as to reduce its potential energy. The expansion rate reduces from exponential to power-law in time. In this sense, a vacuum density in the high-dimensional brane-world can appear as quintessence in the low-energy, 4-d effective theory [67]. Similar arguments can be posed for general supergravity theories without invoking higher dimensions. Although none of these arguments are rigorous, they lend support to the quintessence proposal and suggest directions to search for a specific candidate for the quintessence field.

Significant theoretical challenges remain. Obviously, one goal is to identify the quintessence scalar field or to replace the field by some dynamical mechanism. Perhaps a more satisfying solution to the coincidence problem can be found which explains why quintessence could not have dominated at a much earlier epoch. A second issue is whether quintessence induces fifth force effects and time-varying constants which are inconsistent with known experimental constraints [68]. For generic, light scalar fields, a dimensional estimate suggests that the effects would exceed current experimental limits [69]. To avoid the problem, a dimensionless parameter expected to be of order unity would instead have to be set to less than  $10^{-5}$ . Whether this tuning is problematic is a matter of judgment; one must recall that the problem which quintessence addresses is at the  $10^{100}$  level, so perhaps the tuning is acceptable. Or, perhaps the tuning is not needed because the scalar field has suppressed couplings for reasons of symmetry. A third issue is the time-honored question concerning the cosmological constant: if quintessence accounts for the current cosmic acceleration, why is the vacuum density zero ( $\Lambda = 0$ ) or, perhaps, non-zero but much smaller than the quintessence energy density. A fourth issue is whether there is any connection between accelerated expansion of the past (inflation) and the accelerated expansion of the present, as suggested by Peebles and Vilenkin [70]. Finally, the quintessence scenario must be integrated into fundamental theory. In many ways, the list of challenges are similar to the challenges for inflationary cosmology, the cosmic acceleration of the past. Perhaps nature is giving us a message.

I would like to thank Mr. Pritzker for sponsoring a timely and exciting program addressing the key issues in cosmology as we enter the new millennium. His generous support made the event memorable. I would also like to thank the organizers for their tremendous support and hospitality. Fi-

nally, I want to thank the Isaac Newton Institute for Mathematical Sciences for support during the preparation of the manuscript. This research was supported by the US Department of Energy grant DE-FG02-91ER40671 (Princeton).

## References

1. R. R. Caldwell, R. Dave and P. J. Steinhardt, *Phys. Rev. Lett.* **80**, 1582(1998). R. R. Caldwell, R. Dave and P. J. Steinhardt, *Phys. Rev. Lett.* **80**, 1582(1998).
2. A.D. Dolgov, *Pis'ma ZhETF* **41**, 345 (1985). M. Ozer and M.O. Taha, *Phys. Lett. B* **171**, 363 (1986); *Nucl. Phys. B* **287**, 776 (1987); *Phys.Rev.D* **45**, 997 (1992).
3. N. Weiss, *Phys. Lett. B* **197**, 42 (1987); B. Ratra and J.P.E. Peebles, *Astrophys. J.* , 325,L17 (1988); C.Wetterich, *Nucl. Phys. B* **302**, 668 (1988), and *Astron. Astrophys.* **301**, 32 (1995); J.A. Frieman, *et al. Phys. Rev. Lett.* **75**, 2 077 (1995); K. Coble, S. Dodelson, and J. Frieman, *Phys. Rev. D* **55**, 1851 (1995); P.G. Ferreira and M. Joyce, *Phys. Rev. Lett.* **79**, 4740 (1997); *Phys. Rev. D* **58**, 023503 (1998). 1582
4. A. Einstein, *Sitz. Preuss. Akad. Wiss.* **142**, (1917).
5. A.H. Guth, *Phys. Rev. D* **23**, 347 (1981).
6. A. D. Linde, *Phys. Lett.* **108B**, 389 (1982).
7. A. Albrecht and P. J. Steinhardt, *Phys. Rev. Lett.* **48**, 1220 (1982).
8. For an introduction to inflationary cosmology, see A. H. Guth and P. J. Steinhardt, "The Inflationary Universe" in **The New Physics**, ed. by P. Davies, (Cambridge U. Press, Cambridge, 1989) pp. 34-60.
9. For a recent review, see N. Bahcall, J.P. Ostriker, S. Perlmutter and P.J. Steinhardt, *Science*, 284, 1481 (1999).
10. S. Perlmutter, *et al.*, LBL-42230 (1998), astro-ph/9812473; S. Perlmutter, *et al.*, *Astrophys. J.* (**in press**),astro-ph/9812133.
11. A.G. Riess, *et al.*, *Astrophys. J.* **116**,, 1009(1998).
12. P. M. Garnavich, *et al.*, *Astrophys. J.* **509**,, 74(1998).
13. S. Perlmutter, M. S. Turner and M. White, *Astrophys. J.* (**submitted**),, astro-ph/9901052,(1999).
14. S. Perlmutter, *et al.*, *Astrophys. J.* **483**,, 565(1997).
15. S. Perlmutter, *et al.*, 1995. LBL-38400, page I.1 (1995); also published in *Thermonuclear Supernovae*, P. Ruiz-Lapuente, R. Canal and J.Isern, editors, Dordrecht: Kluwer, page 749 (1997)
16. P. Garnavich, *et al.*, *Astrophys. J.* **493**,, L53(1998)
17. B.P. Schmidt, *et al.*, *Astrophys. J.* **507**,, 46(1998)
18. A.G. Riess, A.V. Filippenko, W. Li, B.P. Schmidt, astro-ph/9907038.stroph/9907038
19. J. P. Ostriker and P. J. Steinhardt, *Nature* **377**, 600 (1995).
20. L. Wang, R. Caldwell, J.P. Ostriker and P.J. Steinhardt, *Astrophys. J.* (**submitted**),, astro-ph/9901388,(1999).
21. B. Chaboyer, *et al. Astrophys. J.* **494**,, 96(1998).
22. M. Salaris & A. Weiss, *Astron. Astrophys.* **335**, 943 (1998).
23. R.H. Dicke and P.J.E. Peebles, in *General Relativity: An Einstein Centenary Survey*, ed. by S.W. Hawking and W. Israel, (Cambridge: Cambridge U. Press, 1979), pp. 504-517.
24. For an introduction to the CMB power spectrum and its interpretation see, P.J. Steinhardt, "Cosmology at the Crossroads", *Particle and Nuclear Astrophysics and Cosmology in the Next Millenium*, ed. by E.W. Kolb and P.

- Peccei (World Scientific, Singapore, 1995), pp. 51-72.
25. The physics of CMB anisotropy generation is discussed in W. Hu, N. Sugiyama and J. Silk, *Nature* **386**, 37 (1997).
  26. M. Kamionkowski, D. N. Spergel, N. Sugiyama, *Astrophys. J.* **426**, L57(1994).
  27. A. Miller *et al.*, astro-ph/9906421
  28. G.F. Smoot, *et al.*, *Astrophys. J.* **396**, L1(1992); C. L. Bennett *et al.*, *Astrophys. J.* **464**, L1(1996).
  29. S.R. Platt *et al.*, *Astrophys. J.* **475**, L1(1997).
  30. E. S. Cheng, *et al.*, *Astrophys. J.* **488**, L59(1997).
  31. M. J. Devlin, *et al.*, *Astrophys. J.* **509**, L69(1998); T. Herbig, *et al.*, *Astrophys. J.* **509**, L73(1998); A. Oliveira-Costa, *et al.*, *Astrophys. J.* **509**, L77(1998)
  32. B. Netterfield, M.J. Devlin, N. Jarosik, L. Page and E.L. Wallack, *Astrophys. J.* **474**, 47(1997).
  33. P. F. Scott, *et al.*, *Astrophys. J.* **461**, L1(1996).
  34. E. M. Leitch, A.C.S. Readhead, T.J. Pearson, S.T. Myers and S. Gulkis, *Astrophys. J.* **518**, (1999), astro-ph/9807312, (1998).
  35. R. Caldwell and P.J. Steinhardt, in *Proceedings of the Non-sleeping Universe Conference*, ed. by T. Lago and A. Blanchard (Kluwer Academic, 1998).
  36. R. Dave, U. of Penn. Ph.D. thesis (1999).
  37. A. Vilenkin, *Phys. Rev. Lett.* **53**, 1016 (1984).
  38. D. Spergel & U.-L. Pen, *Astrophys. J.* **491**, L67(1996).
  39. M.P. Bronstein, *Phys. Zeit. der Sowjetunion* **3**, 73 (1933).
  40. J. Bardeen, P. J. Steinhardt and M. S. Turner, *Phys. Rev. D* **28**, 679 (1983).
  41. A. H. Guth and S.-Y. Pi, *Phys. Rev. Lett.* **49**, 1110 (1982).
  42. A. A. Starobinskii, *Phys. Lett. B* **117**, 175 (1982).
  43. S. W. Hawking, *Phys. Lett. B* **115**, 295 (1982).
  44. P.J. Steinhardt and R. Caldwell, "Introduction to Quintessence," in **Cosmic Microwave Background and Large Scale Structure of the Universe**, ed. by Y.-I. Byun and K.-W. Ng, (Astronomical Society of the Pacific, 1998), pp. 13-21.
  45. R. Caldwell and P.J. Steinhardt, *Phys. Rev. D* **57** 6057 (1998).
  46. L. Wang and P.J. Steinhardt, *Astrophys. J.* **508**, 483(1998).
  47. R. Caldwell, R. Juskiwicz, P.J. Steinhardt and P. Bouchet, in preparation (1999).
  48. W. Hu, D.J. Eisenstein, M. Tegmark, M. White, *Phys. Rev. D* **59**, 023512 (1999).
  49. I. Zlatev, L. Wang, R. Caldwell, and P.J. Steinhardt, to appear.
  50. G. Huey, L. Wang, R. Dave, R. Caldwell, and P.J. Steinhardt, *Phys. Rev. D* **59**, 063005 (1999).
  51. I. Zlatev, L. Wang and P.J. Steinhardt, *Phys. Rev. Lett.* **82**, 896-899 (1999).
  52. P.J. Steinhardt, L. Wang and I. Zlatev, *Phys. Rev. D* **59**, 123504 (1999).
  53. I. Zlatev and P.J. Steinhardt, to appear *Phys. Lett.* (1999).
  54. R. Dave, Ph.D. thesis, U. of Penn. (1999).
  55. B. Ratra and J.P.E. Peebles, *Astrophys. J.* **325**, L17 (1988); B. Ratra, and P.J.E. Peebles, *Phys. Rev. D* **37**, 3406 (1988).
  56. G. Huey and P.J. Steinhardt, in preparation.
  57. I. Affleck, *et al.*, *Nucl Phys B* **256**, 557 (1985).
  58. C. Hill, and G.G. Ross, *Nuc Phys B* **311**, 253 (1988).
  59. C. Hill and G.G. Ross, *Phys Lett B* **203**, 125 (1988).
  60. P. Binetruy, M. K. Gaillard, and Y.-Y. Wu, *Nucl Phys B* **481**, 109 (1996).
  61. T. Barreiro, B. Carlos, and E. J. Copeland, *Phys. Rev. D* **57**, 7354 (1998).
  62. P. Binetruy, *Phys. Rev. D* **60**, 063502 (1999).
  63. S. Perlmutter, M.S. Turner, and M. White, *Phys. Rev. Lett.* **83**, 670 (1999).

64. G. Efstathiou, astro-ph/9904356.
65. S. Podariou and B. Ratra, KSUPT-99/6
66. T.D. Saini, S. Raychaudhury, V. Sahni, A.A. Starobinsky, astro-ph/9910231.
67. P. Steinhardt, to appear in *Phys. Lett. B*, hep-th/9907080.
68. S. Carroll, *Phys. Rev. Lett.* **81** 3067 (1998).
69. For a review, see T. Damour, *Class. Quant. Grav.* **13**, 133 (1996); also, *Proceedings of the 5th Hellenic School of Elementary Particle Physics*, gr-qc/9606079.
70. P.J.E. Peebles and A. Vilenkin, *Phys. Rev. D***59** 063505 (1999).